J. Fluid Mech. (1984), vol. 141, pp. 265–274
Printed in Great Britain

Refraction–diffraction model for weakly nonlinear water waves

By PHILIP L.-F. LIU AND TING-KUEI TSAY
School of Civil and Environmental Engineering, Cornell University, Ithaca, NY 14853

(Received 26 April 1983 and in revised form 6 September 1983)

A model equation is derived for calculating transformation and propagation of Stokes waves. With the assumption that the water depth is slowly varying, the model equation, which is a nonlinear Schrödinger equation with variable coefficients, describes the forward-scattering wavefield. The model equation is used to investigate the wave convergence over a semicircular shoal. Numerical results are compared with experimental data (Whalin 1971). Nonlinear effects, which generate higher-harmonic wave components, are definitely important in the focusing zone. Mean free-surface set-downs over the shoal are also computed.

1. Introduction

The parabolic approximation method has been developed extensively for studying forward-scattering problems in water waves in the last five years. Based on a linear water-wave theory, Radder (1979) and Lozano & Liu (1980) showed that the diffraction effects of a slowly varying refractive index can be described by a linear Schrödinger equation. Tsay & Liu (1982), Liu & Tsay (1983*a*) and Berkhoff, Booy & Rodder (1982) developed numerical algorithms to the Schrödinger equation for obliquely incident waves over varying topographies. Tsay & Liu (1982) also calculated the wavefield in the neighbourhood of a thin breakwater on a sloping bottom. These numerical results compared reasonably well with available experimental data. Based on the same linear formulation, Liu & Tsay (1983*b*) extended the theory to include backward scattering (reflection) via an iterative procedure.

Whalin (1971), in his wave-tank experiments concerning wave refraction over a semicircular sloping topography (which acts as a focusing lens), observed that in the region of wave convergence the nonlinear effects became important. A significant amount of wave energy was transferred from the fundamental-frequency component to the higher-harmonic components owing to nonlinearity. The linear theories mentioned above fail to give the appropriate description of this problem. In this paper we present a refraction–diffraction model based on the Stokes-wave theory. Assuming that the bottom slope is smaller than the wave slope ka and maintaining the accuracy up to $O(ka)^2$, we derive an evolution equation for the wave envelope which is a nonlinear Schrödinger equation with variable coefficients. This evolution equation is an extension to the constant-water-depth case (Yue & Mei 1980) and to the one-dimensional problem (Djordjevic & Redekopp 1978). The parabolic approximation is then applied to expedite numerical computations. A portion of Whalin's experimental data is used to verify the present model. Despite the existence of scatterings in experimental data, a reasonably good agreement between experimental results and the present theory is observed for the cases when the Ursell parameter is less than unity. The mean free-surface set-down due to wave shoaling is also calculated. For

the cases where the Ursell parameter is large, the present theory becomes inapplicable and the Boussinesq equations should be used as the theoretical base. This part of the results will be presented in a separate paper.

2. Model equations

The description of the transformation of two-dimensional Stokes waves over a seabed of mild slope varying only in the direction of wave propagation is first given by Djordjevic & Redekopp (1978). Using the multiple-scale variable with an assumption that the percentage change of water depth within one wavelength, $O(|\nabla h|/kh) = O(\delta)$, is one order smaller than the slope of the free surface, i.e. $O(\delta) = O(ka)^2$, and following a perturbation analysis similar to those developed by Chu & Mei (1970) and Davey & Stewartson (1974), Djordjevic & Redekopp showed that the evolution equation for the leading-order wave amplitude $A(x, t)$ is a nonlinear Schrödinger equation. The derivation of the evolution equation for three-dimensional cases where the bottom profile also varies slowly in the direction normal to that of wave propagation is straightforward but lengthy. The details of the derivation will not be presented here. For second-order Stokes waves propagating primarily in the x-direction, the evolution equation is

$$2\mathrm{i}\bar{k}\frac{\partial A}{\partial x}+\nabla^2 A+\left[k^2-\bar{k}^2-\frac{\nabla^2(CC_g)^{\frac{1}{2}}}{(CC_g)^{\frac{1}{2}}}+\mathrm{i}\frac{\partial \bar{k}}{\partial x}\right]A-\frac{K|A|^2A}{(CC_g)^2}=\frac{1}{CC_g}\frac{\partial^2 A}{\partial t^2}-\frac{2\mathrm{i}\omega_0}{CC_g}\frac{\partial A}{\partial t}, \tag{2.1}$$

where $a = A/(CC_g)^{\frac{1}{2}}$ is the leading-order wave amplitude, and the free-surface profile can be expressed as

$$\zeta(x,y,t)=\frac{1}{2}\left[\frac{A}{(CC_g)^{\frac{1}{2}}}\exp\mathrm{i}\left(\int^x \bar{k}(x)\,\mathrm{d}x-\omega_0 t\right)+\text{c.c.}\right]+\frac{k}{CC_g}\left\{-\frac{|A|^2}{2\sinh 2kh}\right.$$
$$\left.+\frac{\cosh kh\,(2\cosh^2 kh+1)}{8\sinh^3 kh}\left[A^2\exp 2\mathrm{i}\left(\int^x \bar{k}(x)\,\mathrm{d}x-\omega_0 t\right)+\text{c.c.}\right]\right\}+O(ka)^3 \tag{2.2}$$

up to second order in ka, where c.c. represents the complex conjugate. It is understood that the coordinates used in (2.1) are slow coordinates. In both (2.1) and (2.2), $\bar{k}$ denotes the wavenumber associated with the modified topography $\bar{h}(x)$, where the real topography is given as

$$z=-h(x,y)=-[\bar{h}(x)+\tilde{h}(x,y)]; \tag{2.3}$$

here $\bar{h}(x)$ is also a slowly varying function of x. Thus $\bar{k}$ and k are the positive real roots of the transcendental equations

$$\omega_0^2=g\bar{k}\tanh\bar{k}\bar{h},\quad \omega_0^2=gk\tanh kh \tag{2.4}$$

respectively. Lozano & Liu (1980) showed that the choice of $\bar{h}$ must satisfy the condition $k^2-\bar{k}^2=O(\delta^{\frac{4}{3}})$. In (2.1) C and C_g are the local phase and group velocities of waves with frequency ω_0, and the coefficient K for the nonlinear term can be given as

$$K=k^4C^2\frac{[\cosh 4kh+8-2\tanh^2 kh]}{8\sinh^4 kh}. \tag{2.5}$$

In a slightly different form, the evolution equation (2.1) has also been derived independently by Kirby & Dalrymple (1983).

For a quasi-steady-state problem the timescale for the amplitude A is longer than $O(\delta^{-1})$, and (2.1) can be reduced to

$$2i\bar{k}\frac{\partial A}{\partial x}+\nabla^2 A+\left[k^2-\bar{k}^2-\frac{\nabla^2(CC_g)^{\frac{1}{2}}}{(CC_g)^{\frac{1}{2}}}+i\frac{\partial \bar{k}}{\partial x}\right]A-\frac{K|A|^2A}{(CC_g)^2}=0. \tag{2.6}$$

In the limiting case where the water depth is a constant, $k=\bar{k}$ and C, C_g and $\bar{k}$ are constants. Equation (2.6) becomes

$$2i\bar{k}\frac{\partial A}{\partial x}+\nabla^2 A-\frac{K|A|^2A}{(CC_g)^2}=0, \tag{2.7}$$

which is the same equation as that derived by Yue & Mei (1980). On the other hand, if the nonlinear effects are not important, the last term in (2.6) can be ignored. The linear version of (2.6) is the same as that found in Lozano & Liu (1980).

Now we employ the usual parabolic approximation, which assumes that the amplitude envelope varies more slowly in the direction of wave propagation than in the lateral direction, i.e.

$$O\left(\frac{\partial^2}{\partial y^2}\right)\gg O\left(\frac{\partial^2}{\partial x^2}\right),\quad O\left(\bar{k}\frac{\partial}{\partial x}\right)=O\left(\frac{\partial^2}{\partial y^2}\right). \tag{2.8}$$

Equation (2.6) can be simplified to be

$$2i\bar{k}\frac{\partial A}{\partial x}+\frac{\partial^2 A}{\partial y^2}+\left[k^2-\bar{k}^2-\frac{\nabla^2(CC_g)^{\frac{1}{2}}}{(CC_g)^{\frac{1}{2}}}+i\frac{\partial \bar{k}}{\partial x}\right]A-\frac{K|A|^2A}{(CC_g)^2}=0, \tag{2.9}$$

which is a nonlinear Schrödinger equation with x as a timelike variable. In essence, we have converted the elliptic equation (2.6) into a parabolic equation (2.9), which can be solved numerically with efficiency. We remark here that the term $\nabla^2(CC_g)^{\frac{1}{2}}$ is kept in (2.1) for completeness. Since this term is proportional to the curvature of the bottom topography, it does not have to be small even for mild-slope cases.

3. Wave focusing due to bottom topography

Whalin (1971) conducted a series of laboratory experiments concerning wave convergence over a bottom topography that acts as a focusing lens. The wave tank used in the experiments has the horizontal dimensions 25.603 m × 6.096 m. In the middle portion of the wave tank, 7.62 m $< x <$ 15.24 m, eleven semicircular steps were evenly spaced and led to the shallower portion of the channel (figure 1). The equations approximating the topography are given as follows (Whalin 1971):

$$h(x,y)=\begin{cases}0.4572 & (0\leqslant x\leqslant 10.67-G(y)),\\ 0.4572+\frac{1}{25}(10.67-G-x) & (10.67-G\leqslant x\leqslant 18.29-G),\\ 0.1524 & (18.29-\mathrm{G}\leqslant x\leqslant 21.34),\end{cases} \tag{3.1}$$

where

$$G(y)=[y(6.096-y)]^{\frac{1}{2}}\quad (0\leqslant y\leqslant 6.096). \tag{3.2}$$

In both (3.1) and (3.2) the length variables are measured in metres. The bottom topography is symmetric with respect to the centreline of the wave tank, $y=3.048$ m.

A wavemaker was installed at the deeper portion of the channel where the water depth h_0 is 0.4572 m. Three sets of experiments were conducted by generating waves with wave periods $T=1$, 2 and 3 s respectively. Different wave amplitudes were generated for each wave period. In table 1 we summarize the experimental information,

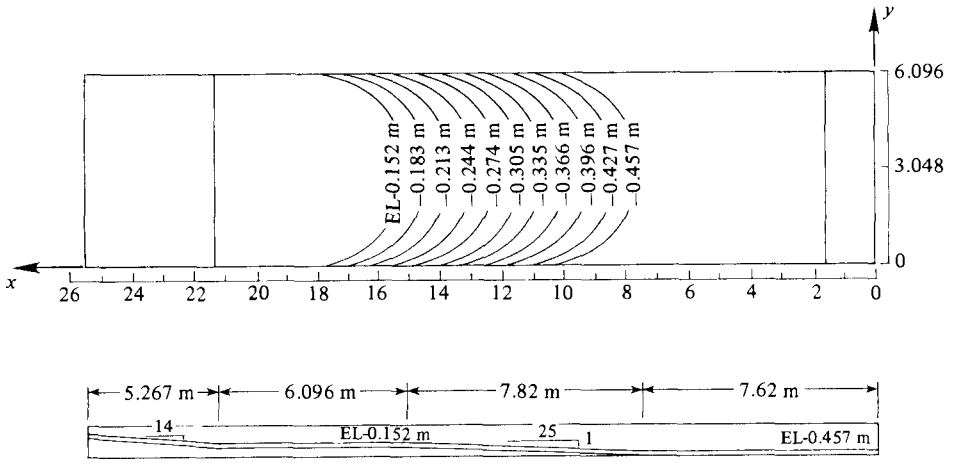

FIGURE 1. Wave-tank configuration.

Wave period T (s)	$k_0 h_0$	Wave amplitude a_0 (cm)			$k_0 a_0$			Ursell parameter U_r		
		(1)	(2)		(1)	(2)		(1)	(2)	
1.0	1.922	0.97	1.95	—	0.041	0.082	—	0.0057	0.0115	—
		(3)	(4)	(5)	(3)	(4)	(5)	(3)	(4)	(5)
2.0	0.735	0.75	1.06	1.49	0.012	0.017	0.024	0.0303	0.0429	0.0603
		(6)	(7)	(8)	(6)	(7)	(8)	(6)	(7)	(8)
3.0	0.468	0.68	0.98	1.46	0.007	0.010	0.015	0.0678	0.0977	0.1456

TABLE 1. Experimental information at water depth $h_0 = 0.4572$ m

including the measured wave amplitude a_0, wave slope $k_0 a_0$ and $k_0 h_0$, near the wavemaker. The Ursell parameter

$$U_r = \frac{a/h}{(kh)^2} \tag{3.3}$$

is also calculated for each experiment. The values of wave slope and Ursell parameter are quite small near the wavemaker, indicating that the nonlinearity is not important at this stage. However, as is evident from Whalin's experiments, waves converged over the semicircular steps and a cusped caustic was formed in the shallower constant-water-depth ($h_1 = 0.1524$ m) region. Moreover, higher-harmonic components are measurable in this region, signalling the importance of nonlinearity. The experimental information near the cusped caustic is also summarized in table 2, in which a_1 is the measured first-harmonic wave amplitude and Σa represents the summation of first- and higher-harmonic amplitudes. Since the Stokes-wave theory becomes inadequate when the Ursell parameter is greater than unity, and the present theory also requires that the bottom slope (which is roughly 0.04 in Whalin's experiments) be smaller than the wave slope, we decided to compare the experimental results from tests (1)–(4), as defined in tables 1 and 2, with the present theory.

Wave period T (s)	$k_1 h_1$	Measured wave amplitude $a_1/\Sigma a$ (cm)			$k_1 a_1/\Sigma k_1 a$			Ursell parameter U_r		
		(1)	(2)		(1)	(2)			(1)	(2)
1.0	0.873	1.72/2.07	2.70/3.50		0.098/0.119	0.155/0.200			0.148/0.178	0.232/0.301
		(3)	(4)	(5)	(3)	(4)	(5)	(3)	(4)	(5)
2.0	0.402	1.20/1.70	1.60/2.60	1.80/4.00	0.032/0.045	0.042/0.069	0.047/0.106	0.487/0.690	0.649/1.055	0.731/1.623
		(6)	(7)	(8)	(6)	(7)	(8)	(6)	(7)	(8)
3.0	0.264	0.90/1.90	1.10/2.40	1.50/3.30	0.016/0.033	0.019/0.042	0.026/0.057	0.846/1.786	1.034/2.256	1.410/3.102

TABLE 2. Experimental information at water depth $h_1 = 0.1524$ m

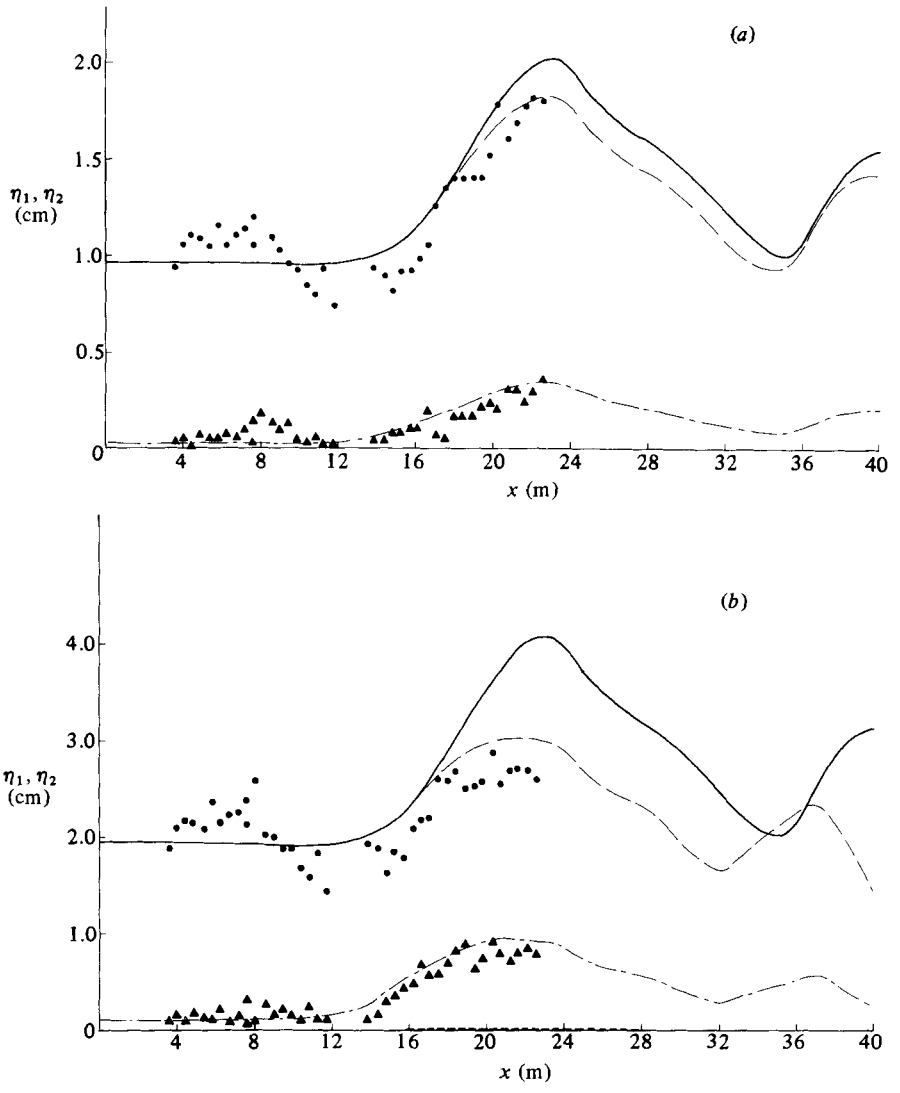

FIGURE 2 (*a*, *b*). For caption see facing page.

To solve the problem by parabolic approximation, we chose the modified bottom topography $\bar{h}(x)$ as follows:

$$\bar{h}(x) = \begin{cases} 0.4572 & (0 \leqslant x \leqslant 7.62), \\ 0.4572 - \frac{1}{25}(x - 7.62) & (7.62 \leqslant x \leqslant 15.24), \\ 0.1524 & (15.24 \leqslant x \leqslant 21.34). \end{cases} \tag{3.4}$$

Owing to the symmetry of the problem, only one-half of the wave tank is involved in the numerical computations ($0 \leqslant y \leqslant 3.048$ m). The governing equation (2.6) is solved numerically by the Crank–Nicholson method (see e.g. Tsay & Liu 1982). The x-coordinate coinciding with the direction of wave propagation is treated as a timelike variable. Solutions are therefore obtained by marching in the x-direction. The nonlinear term in (2.6) is linearized by using Newton's iterative method (Smith 1978,

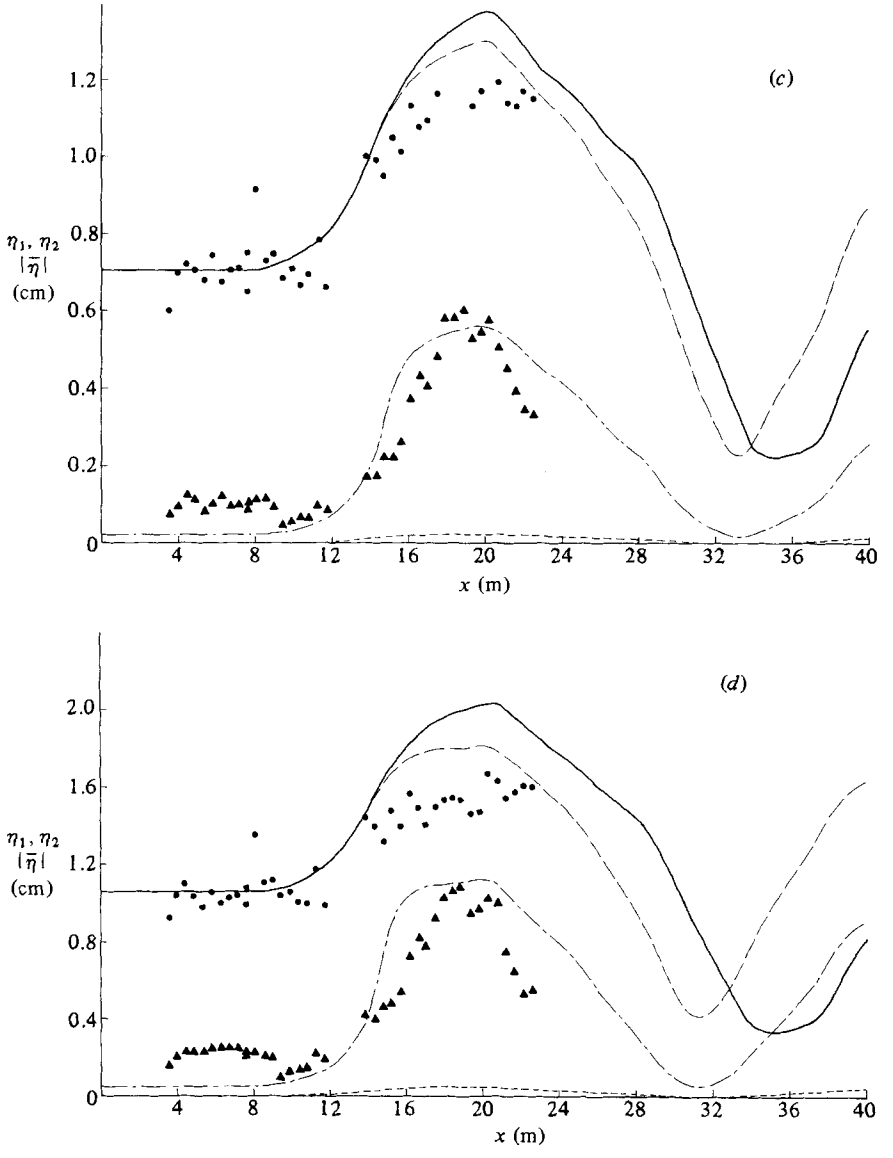

FIGURE 2. Theory *vs.* experimental data (Whalin 1971): ●, ▲, measured first- and second-harmonic amplitudes; ——, linear theory for first-harmonic amplitudes; – – –, η_1, nonlinear theory for first-harmonic amplitude; – – – –, η_2, nonlinear theory for second-harmonic amplitude; - - - - - - - - - -, $|\bar{\eta}|$, nonlinear theory for the mean free-surface set-down. (*a*) $T = 1$ s, $k_0 a_0 = 0.041$; (*b*) 1 s, 0.082; (*c*) 2 s, 0.012; (*d*) 2 s, 0.017.

p. 49). The iteration procedure is stopped and converged solutions are obtained when the relative error between two successive solutions is less than 10^{-4}; i.e. $|A^{(n)} - A^{(n-1)}|/|A^{(n)}| < 10^{-4}$ for $0 \leqslant y \leqslant 3.048$ along a given x-section. The following no-flux boundary conditions are used along the centreline and the sidewall of the tank:

$$\frac{\partial A}{\partial y} = 0 \quad (y = 0, 3.048). \tag{3.5}$$

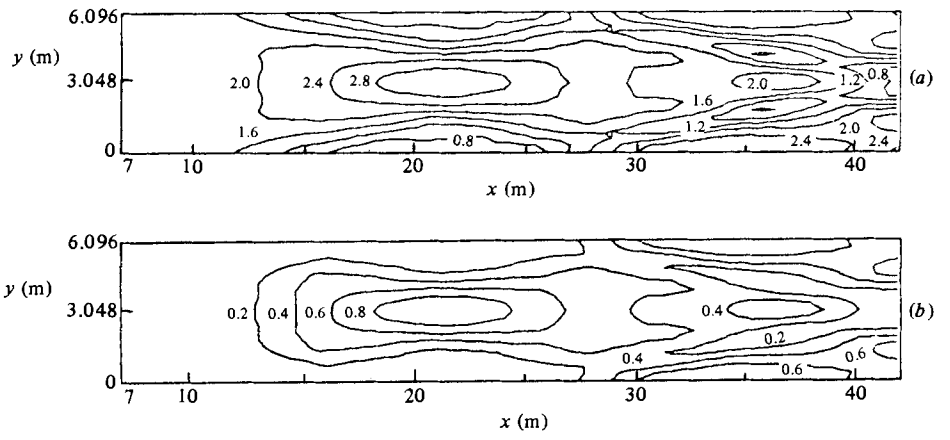

FIGURE 3. (*a*) Contours of the first-harmonic wave amplitude for $T = 1$ s, $k_0 a_0 = 0.082$, (*b*) Contours of the second-harmonic wave amplitude.

For each experimental test, the wave amplitude at $x = 0$ is estimated from the experimental data directly and is used as the initial condition for numerical computations. Owing to the data scattering, an average value is always used.

To ensure that numerical solutions are not sensitive to the choice of grid sizes, different grid sizes are tested. We find that the largest grid size that should be used in the computations is dependent on the desirable resolution of the wavefield in the direction normal to the wave propagation. For the present problems, we use at least 11 points along each x-section. In all the numerical solutions presented here, $\Delta x = 0.3275$ m and $\Delta y = 0.3048$ m are used. In all these computations, two or three iterations are necessary to satisfy the convergency condition.

In figure 2 the numerical results of the wave amplitudes for the first two harmonics along the centreline of the wave tank are compared with experimental data. In these figures the first-harmonic wave amplitude is denoted as η_1, the second-harmonic wave amplitude as η_2 and the second-order mean free-surface set-down as $\bar{\eta}$. Using (2.2), these quantities are defined as

$$\eta_1 = \left| \frac{A}{(CC_g)^{\frac{1}{2}}} \right|, \tag{3.6a}$$

$$\eta_2 = \frac{k}{CC_g} |A|^2 \frac{\cosh kh\,(2\cosh^2 kh + 1)}{4\sinh^3 kh}, \tag{3.6b}$$

$$\bar{\eta} = -\frac{k|A|^2}{2CC_g \sinh 2kh}. \tag{3.6c}$$

For convenience the absolute value of the set-down is plotted. In the case of $T = 1$ s the set-down is very small and can be ignored (figures 2*a*, *b*). For the purpose of comparison, the results from a linear theory (Lozano & Liu 1980) are also presented in the same figures. In spite of the data scattering, the agreement between the nonlinear theory and experimental results is reasonably good. Both the first- and second-harmonic wave amplitudes grow rather rapidly behind the sloping lens. The focusing distance is shorter for longer waves ($T = 2$ s). The linear theory tends to overpredict the first-harmonic wave amplitude, and is of course unable to calculate the second-harmonic component, which is significant in the present cases. The mean

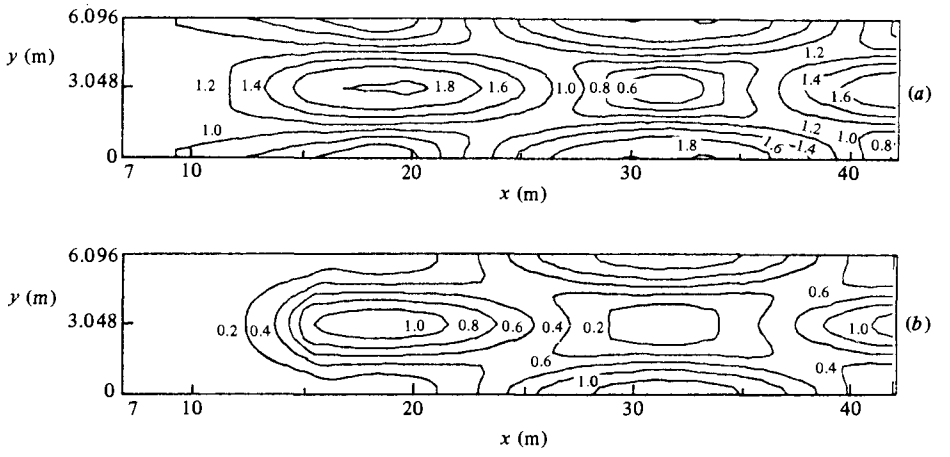

FIGURE 4. (*a*) Contours of the first-harmonic wave amplitude for $T = 2$ s, $k_0 a_0 = 0.017$. (*b*) Contours of the second-harmonic wave amplitude.

free-surface set-downs over the shoaling zone are also evident in the figures. Whalin (1971) reported that there is a very small amount of wave damping (roughly 3 % in the wave tank) caused by the viscous boundary layers along the sidewalls and the bottom of the wave tank. In the numerical results, viscous wave damping is ignored. It is also evident from figure 2 that there appears to be a weak reflection from the slope, which cannot be described properly by the present theory.

In figures 3 and 4 we present the contour lines of the first-harmonic wave amplitude η_1 and the second-harmonic wave amplitude η_2 for experimental tests 2 and 4 respectively. In both cases, it is clear that waves first converge behind the semicircular shoal and bounce between two sidewalls while they propagate down the tank. For longer waves ($T = 2$ s, figure 3) the focus of the wave convergence is sharper and the standing wave pattern is clearly defined. Owing to the appearance of the sidewalls, the existence of wave jumps as discussed by Peregrine (1983) and Kirby & Dalrymple (1983) is not clear in the present examples. This phenomenon deserves further studies, however.

4. Concluding remarks

In this paper we have presented a model describing the propagation and transformation of Stokes waves over a mildly varying topography. The present model is verified by comparing the numerical results with laboratory experimental data. The model can, however, be improved and extended in two directions: (1) the relaxation of the requirement on the smallness of bottom slope as compared with the wave slope is desirable for some practical engineering problems; (2) the extension of the present theory into the shallow-water regime where the Ursell parameter is greater than unity is possible by using the Boussinesq equations as governing equations. Research on the latter aspect is underway; some of the results will be presented in the near future.

This research was supported in part by the New York Sea Grant Institute under a grant to Cornell University. The authors would like to express their appreciation to Dr Robert A. Dalrymple, Dr James T. Kirby and Dr Robert Whalin for their stimulating discussions on the subject.

REFERENCES

BERKHOFF, J. C. W., BOOY, N. & RADDER, A. C. 1982 Verification of numerical wave propagation models for simple harmonic linear water waves. *Coastal Engng* **6**, 255–279.

CHU, V. H. & MEI, C. C. 1970 On slowly-varying Stokes waves. *Rep.* 125, *Water Resources and Hydrodyn. Lab., Dept Civ. Enging, MIT.*

DAVEY, A. & STEWARTSON, K. 1974 On three-dimensional packets of surface waves. *Proc. R. Soc. Lond.* A **338**, 101–110.

DJORDJEVIC, V. D. & REDEKOPP, L. G. 1978 On the development of packets of surface gravity waves moving over an uneven bottom. *Z. angew. Math. Phys.* **29**, 950–962.

KIRBY, J. T. & DALRYMPLE, R. A. 1983 A parabolic equation for the combined refraction–diffraction of Stokes waves by mildly varying topography. *J. Fluid Mech.* **136**, 453–466.

LIU, P. L.-F. & TSAY, T.-K. 1983*a* Water-wave motion around a breakwater on a slowly varying topography. In *Proc. Coastal Structures '83, Specialty Conf. ASCE* (ed. J. R. Weggel), pp. 974–987. ASCE.

LIU, P. L.-F. & TSAY, T.-K. 1983*b* On weak reflection of water waves. *J. Fluid Mech.* **131**, 59–71.

LOZANO, C. & LIU, P. L.-F. 1980 Refraction–diffraction model for linear surface water waves. *J. Fluid Mech.* **101**, 705–720.

PEREGRINE, D. H. 1983 Wave jumps and caustics in the propagation of finite-amplitude water waves. *J. Fluid Mech.* **136**, 435–452.

RADDER, A. C. 1979 On the parabolic equation method for water-wave propagation. *J. Fluid Mech.* **95**, 159–176.

SMITH, G. D. 1978 *Numerical Solution of Partial Differential Equations: Finite Difference Methods*, 2nd edn. Oxford University Press.

TSAY, T.-K. & LIU, P. L.-F. 1982 Numerical solution of water wave refraction and diffraction problems in the parabolic approximation. *J. Geophys. Res.* **87**, 7932–7940.

WHALIN, R. W. 1971 The limit of applicability of linear wave refraction theory in a convergence zone. *Res. Rep.* H-71-3, *U.S. Army Corps of Engrs, Waterways Expt Station, Vicksburg, MS.*

YUE, D. K. P. & MEI, C. C. 1980 Forward diffraction of Stokes waves by a thin wedge. *J. Fluid Mech.* **99**, 33–52.